Synchronization Stability Analysis Under Ultra-Weak Grid Considering Reactive Current Dynamics

Hu, Bin; Zhan, Ling; Sahoo, Subham; Chen, Liang; Nian, Heng; Blaabjerg, Frede

Published in:
I E E E Transactions on Industrial Electronics

DOI (link to publication from Publisher):
10.1109/TIE.2024.3370947

Publication date:
2024

Document Version
Accepted author manuscript, peer reviewed version

Synchronization Stability Analysis under Ultra-Weak Grid considering Reactive Current Dynamics

Bin Hu, *Member, IEEE*, Ling Zhan, Subham Sahoo, *Senior Member, IEEE*,
Liang Chen, Heng Nian, *Senior Member, IEEE*, Frede Blaabjerg, *Fellow, IEEE*

***Abstract*—The synchronization stability of grid-following converter (GFC) has attracted extensive attention. It has been reported that the transient synchronization behavior during a grid fault is dominated by the phase-locked loop (PLL), while the current loop is always approximated as a unity gain. Nevertheless, this letter notices that the reactive current dynamics will also influence the synchronization stability under ultra-weak grid, which increases the risk of losing synchronization, and causes the PLL output frequency to be outside the limitation. Accordingly, a refined fourth-order model is proposed to reveal the above underlying mechanism and quantify this coupling effect.**

***Index Terms*—Grid-following converter, phase-locked loop, synchronization stability, ultra-weak grid, current dynamics.**

I. Introduction

The renewable energy sources are typically interfaced to the grid via grid-following converter (GFC), and rely on the phase-locked loop (PLL) to implement synchronization [1].

If the grid is under large disturbances such as a grid voltage sag, the PLL cannot accurately track the grid phase during the variation of operation points [2]. Then, GFC will lose synchronization stability, which severely challenges the security of electricity supply [3].

This synchronization dynamic lies in the low-frequency range, while the bandwidth of current controller is usually more than ten times larger than PLL [4]. Therefore, the effect of the current loop can be ignored, such that the transient synchronization model of GFC is ultimately characterized by a second-order differential equation [5]. Based on this model, [6] analyzes that increasing the damping ratio of PLL can enhance the synchronization stability.

Recently, large-scale wind and solar-based generation systems are built in the remote areas, and have to be operated under ultra-weak gird condition [7], i.e., the short circuit ratio (SCR) of transmission line impedance is close to 1. This letter firstly prophesizes that even with a sufficiently large current controller bandwidth, the reactive current is dynamically coupled with the PLL under ultra-weak grid, which causes the misjudgment of synchronization stability range, and triggers the boundary of the PLL output frequency. In addition, continuously increasing the damping ratio of PLL will deteriorate the synchronization stability under ultra-weak grid.

To this end, a fourth-order transient synchronization model considering reactive current dynamics is proposed in this letter to explain the above phenomena.

II. Traditional Transient Synchronization Model

Fig. 1 illustrates the topology of GFC connected with weak grid, which detects the grid frequency and phase through synchronous reference frame (SRF)-PLL. The subscripts 'd' and 'q' denote the two-phase rotating frame. The superscript * denotes the reference value. $\boldsymbol{U}_{gfc}$, $\boldsymbol{U}_{pcc}$ and $\boldsymbol{U}_{gcp}$ are the three-phase voltage of the GFC, the point of common coupling (PCC) and the grid connection point (GCP), respectively. $\boldsymbol{Z}_g=R_g+j\omega_g L_g$ is the grid impedance. $\omega_g=100\pi$ rad/s is the fundamental angular frequency. θ_{pll} and ω_{pll} are the PLL output angle and angular frequency. $\boldsymbol{I}$ represent the three-phase current. Low-pass filter (LPF) is added in feed-forward compensation to reduce grid harmonics. The GFC provides 2% reactive current per percent of the voltage drop according to grid code. The other circuit and controller parameters are listed in Table I, where the current controller bandwidth is around 1000Hz.

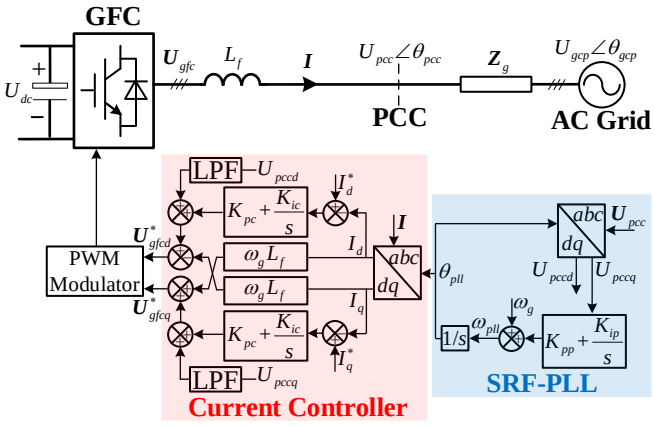

Fig. 1. Topology of grid-following converter connected with weak grid.

TABLE I
Circuit and Controller Parameters

Parameter	Value	Parameter	Value
U_{nom}, Rated Voltage	690 V	U_{dc}, Dc-link voltage	1150 V
P_{nom}, Rated power	1.5 MW	L_f, Filter inductance	0.05 p.u.
K_{pp}, P gain of PLL	0.4	K_{pc}, P gain of current controller	0.3
K_{ip}, I gain of PLL	25	K_{ic}, I gain of current controller	3

This work was supported by the National Natural Science Foundation of China under Grant 52325702. *(Corresponding author: Heng Nian.)*

Bin Hu, Ling Zhan and Heng Nian are with the College of Electrical Engineering, Zhejiang University, Hangzhou, China (e-mail: binhuee@zju.edu.cn, zhanling@zju.edu.cn, nianheng@zju.edu.cn).
Subham Sahoo and Frede Blaabjerg are with the Department of Energy, Aalborg University, Aalborg, Denmark (e-mail: sssa@energy.aau.dk, fbl@energy.aau.dk).
Liang Chen with the School of Information Science and Engineering, NingboTech University, Ningbo, China (e-mail: 21410077@zju.edu.cn).

It can define the angle difference δ between θ_{pll} and θ_{gcp} as shown in (1) to characterize the transient synchronization process [5], where the superscript $'$ denotes the differential notation. The GFC will lose synchronization when δ exceeds the maximum angle δ_{max} during a grid fault [3].

$$\delta=\theta_{pll}-\theta_{gcp}=\int\left(K_{pp}+K_{ip}\int\right)\underbrace{\left(-U_{gcp}\sin\delta+R_gI_q+\omega_{pll}L_gI_d+L_gI_q'\right)}_{U_{pccq}} \quad (1)$$

This letter will give some cases that U_{gcp} sags from U_{nom}=1 p.u. to U_{fault} to analyze the synchronization stability of GFC, where the real-time electromagnetic transients (EMT) based simulation studies are carried out in Matlab/Simulink.

- *Case 1*: L_g=0.2 p.u., R_g=0.2 p.u., U_{fault}=0.55 p.u.

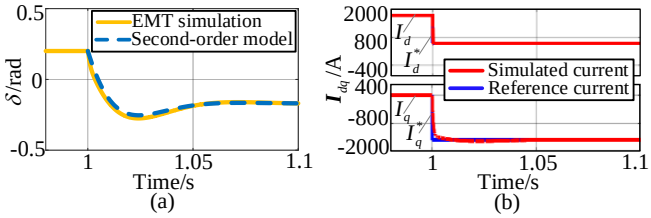

Fig. 2. Dynamic response with grid fault for *Case 1*. (a) angle response. (b) current response.

According to *Case 1*, it can be found that the current reaches a steady state quickly, thus, the GFC can be represented as an ideal controllable current source. In view of (1), the second-order transient synchronization model and its initial value are shown in (2) and (3) [5]. The second-order model matches the EMT simulation quite significantly in Fig. 2 (a).

$$\begin{cases}\left(\delta\right)'=\delta'\\ \left(\delta'\right)'=\dfrac{-K_{pp}U_{fault}\cos\delta\delta'+K_{ip}\left[-U_{fault}\sin\delta+R_gI_q^*+\left(\omega_g+\delta'\right)L_gI_d^*\right]}{1-K_{pp}L_gI_d^*}\end{cases} \quad (2)$$

$$\begin{cases}\delta_i=\sin^{-1}\left(\omega_gL_gI_{max}/U_{nom}\right)\\ \delta_i'=K_{pp}\left(-U_{fault}\sin\delta_i+R_gI_q^*+\omega_gL_gI_d^*\right)/\left(1-K_{pp}L_gI_d^*\right)\end{cases} \quad (3)$$

III. Synchronization Stability Analysis under Ultra-Weak Grid

Under the ultra-weak gird condition, the grid resistance is always much smaller than grid inductance to prevent excessive line losses [8]. Therefore, this Section only accounts for the pure inductive grid as the case study.

According to *Case 2* and *Case 3*, there is a large error between the second-order model and the EMT simulation. Especially in Fig. 4 (a), the second-order model predicts that δ will converge to steady state, while the GFC loses synchronization under ultra-weak grid, and the angle response are in the opposite direction at the first moment. In addition, there is a significant fluctuation of PLL output frequency in Fig. 3 (c). The f_{pll} reaches to 23 Hz during a grid fault, which may trigger the PLL limiter.

- *Case 2*: L_g=0.8 p.u., R_g=0., U_{fault}=0.55 p.u. (ultra-weak grid)

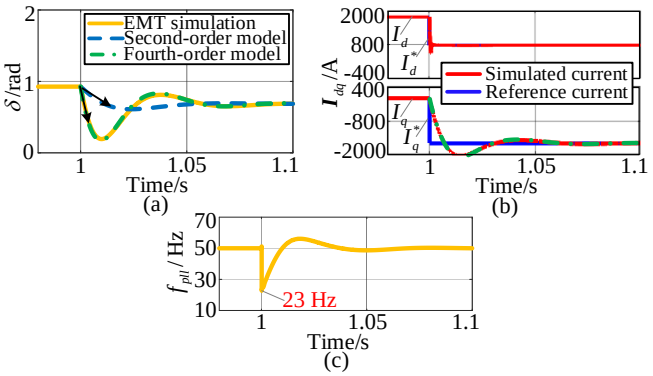

Fig. 3. Dynamic response with grid fault for *Case 2*. (a) angle response. (b) current response. (c) frequency response.

- *Case 3*: L_g=0.8 p.u., R_g=0., U_{fault}=0.75 p.u. (ultra-weak grid)

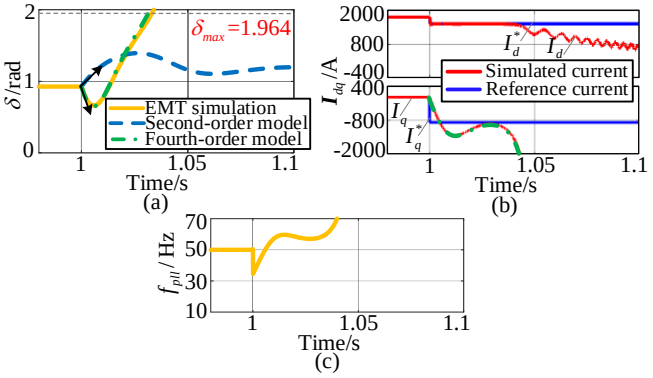

Fig. 4. Dynamic response with grid fault for *Case 3*. (a) angle response. (b) current response. (c) frequency response.

Compared with Fig. 2 (b) and Fig. 3 (b), I_d always converges to the reference value quickly, while the dynamic response of I_q is significantly slower under ultra-weak grid. The reason is that compared with the $\omega_{pll}L_gI_d$ in (1), the differential term L_gI_q' may cause more complex coupling with δ. Therefore, the reactive current dynamic is the potential cause of synchronization stable range misjudgment and the abnormal PLL output frequency.

$$\begin{cases}U_{pccq}=U_{gfcq}-\omega_{pll}L_fI_d-L_fI_q'\\ U_{gfcq}=K_{pc}\left(I_q^*-I_q\right)+K_{ic}\int\left(I_q^*-I_q\right)+\omega_gL_fI_d\end{cases} \quad (4)$$

In order to consider the influence of reactive current, it needs to combine with (1) and the circuit/control equations of (4). Then the fourth-order transient synchronization model considering reactive current dynamics can be elaborated as follow,

$$
\begin{cases}
(\delta)' = \delta' \\
(I_q)' = I_q' \\
(\delta')' = -K_{pp}U_{fault}\cos\delta\delta' + K_{ip}\left[-U_{fault}\sin\delta + (\omega_g+\delta')L_gI_d^* + L_gI_q'\right] \\
\quad + K_{pp}L_g\left[-K_{pc}I_q' + K_{ic}(I_q^* - I_q) + U_{fault}\cos\delta\delta'\right]/(L_g+L_f) \\
(I_q')' = (1-K_{pp}L_gI_d^*)\left[-K_{pc}I_q' + K_{ic}(I_q^* - I_q) + U_{fault}\cos\delta\delta'\right]/(L_g+L_f) \\
\quad -I_d^*\left\{-K_{pp}U_{fault}\cos\delta\delta' + K_{ip}\left[-U_{fault}\sin\delta + (\omega_g+\delta')L_gI_d^* + L_gI_q'\right]\right\}
\end{cases} \tag{5}
$$

$$
\begin{cases}
\delta_i = \sin^{-1}\left(\omega_gL_gI_{max}/U_{nom}\right) \\
I_{qi} = 0 \\
\delta_i' = K_{pp}(-U_{fault}\sin\delta_i + \omega_gL_gI_d^* + L_gI_{qi}')/(1-K_{pp}L_gI_d^*) \\
I_{qi}' = \left[K_{pc}I_q^* + U_{fault}\sin\delta_i + \omega_gL_fI_d^* - (\omega_g+\delta_i')(L_f+L_g)I_d^*\right]/(L_f+L_g)
\end{cases} \tag{6}
$$

Fig. 3 and Fig. 4 depict the δ and I_q according to (5) and (6), which verifies the accuracy of fourth-order model.

Compared with (3), δ_i' in (6) contains the additional L_gI_{qi}' after considering reactive current dynamics. When the reactive current reference changes instantly during a grid fault under ultra-weak grid, L_gI_q' will be a very large negative value, resulting in the initial movement speed of δ increases rapidly and moving downward. In terms of Fig. 3(a) and Fig. 4(a), the slope of δ for EMT simulation at 1 s is larger than ignoring reactive current dynamics, which is more prone to exceed δ_{max} and lose synchronization stability as shown in Fig. 4(a) [5]. Since the PLL output frequency f_{pll} is equal to ($\delta'/2\pi$+50) Hz, f_{pll} will also change abruptly with the rapid movement of δ, which explain the phenomenon that the f_{pll} is outside the limitation in Fig. 3 (c).

Fig. 5 depicts the synchronization stable range with PLL parameter deviations, where the U_{fault}=0.75 p.u., L_g=0.8 p.u. The blue area indicates that the system is synchronization stable.

According to Fig. 5 (a), as the proportional gain of PLL decreases and the integral gain of PLL increases, the damping ratio is reduced, then the risk of losing synchronization is increased. Therefore, the GFC can be stabilized by increasing K_{pp} [6]. However, there is less stable area after considering the reactive current dynamics as shown in Fig. 5 (b). Meanwhile, the GFC will lose synchronization when K_{pp} further increases. The reason is that the degree of coupling between δ and I_q in (5) will become stronger with larger K_{pp}, and the movement speed of δ increases to exceed δ_{max} more easily.

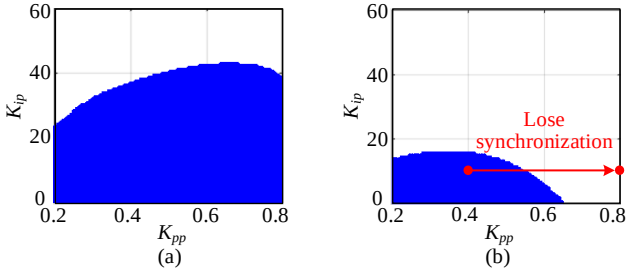

Fig. 5. Synchronization stable range with PLL parameter deviations.
(a) Second-order model ignoring reactive current dynamics.
(b) Fourth-order model considering reactive current dynamics.

In summary, the reactive current dynamics cannot be ignored under ultra-weak grid due to the misjudgment of synchronization stability. And the method in [5] is an optional solution under ultra-weak grid, which introduces an additional reverse angular frequency to slow down the movement of δ to prevent overshoot, rather than only focus on the design of K_{pp} and K_{ip} for damping ratio.

IV. Experimental Results

The experimental results are obtained in the platform of control-hardware-in-loop (CHIL). The 1.5 MW GFC model is developed in Typhoon 602+ with the time step of 1 μs. The control strategies are implemented in the TMS320F28335/Spartan6 XC6SLX16 DSP+FPGA control board. The circuit and controller parameters are the same as Table I.

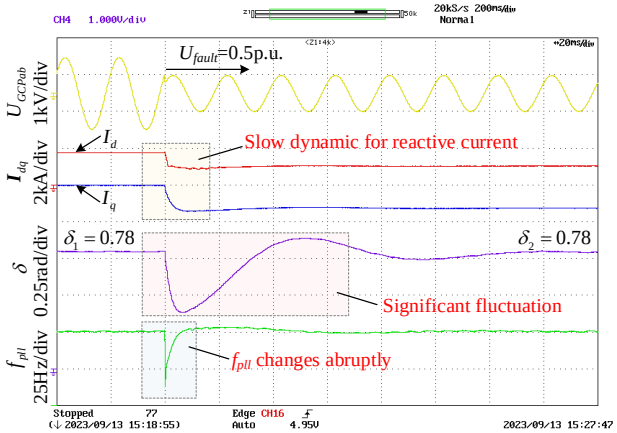

Fig. 6. Experimental results to study the coupling of δ and reactive current (K_{pp}=0.4).

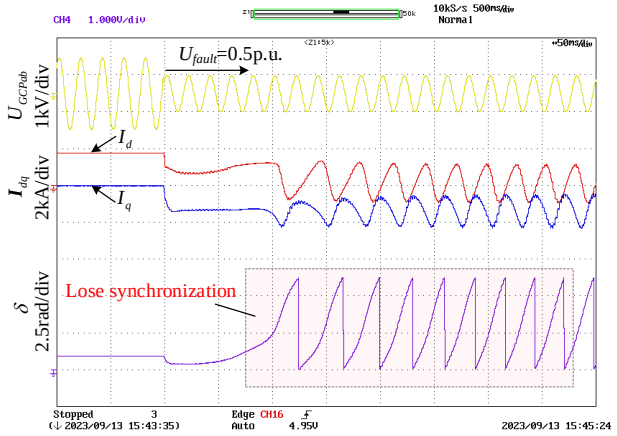

Fig. 7. Experimental results to study the impact of PLL proportional gain on stability (K_{pp}=0.8).

The steady-state value of δ after the fault is given by:

$$
\delta_n = \sin^{-1}\left[\left(\omega_gL_gI_d^* + R_gI_q^*\right)/U_{fault}\right] \tag{7}
$$

To verify the coupling between δ and reactive current, the parameters are set to R_g=0.1 p.u., L_g=0.7 p.u., U_{fault}=0.5 p.u., I_d^* =0.6 p.u., I_q^*=-0.7 p.u. From (6) and (7), it can calculate that δ_i=δ_n=0.78 rad.

According to Fig. 6, the reactive current cannot quickly follow the reference value under ultra-weak grid. At this time, even though the steady-state value of δ keeps the same after grid fault, it will cause large fluctuations due to the coupling with the reactive current. Moreover, the output frequency of the PLL will change abruptly at the moment of fault, which can easily trigger the limiter.

Since the damping ratio of PLL is ξ=sqrt(U_{nom}/K_{ip})K_{pp}/2, the damping ratio can be enhanced when PLL proportional gain K_{pp} increases from 0.4 to 0.8. However, the GFC will lose synchronization stability with larger K_{pp} under ultra-weak grid based on Fig. 7, which validates the conclusion of Fig. 5.

V. Conclusions

When the grid fault occurs under ultra-weak grid, the PLL will dynamically couple with the reactive current during the synchronization process. This letter develops a fourth-order transient model to accurately judge the stable range with parameter deviations. Based on the proposed model, this letter notices that the movement of δ will speed up under ultra-weak grid, leading to loss of synchronization and reaching PLL frequency limitation. At this time, increasing the proportional gain of the PLL to enhance the damping ratio will worsen the synchronization stability.

References

[1] M. Li and H. Nian, "Perturbation amplitudes design method based on confidence interval evaluation for impedance measurement," *IEEE Trans. Ind. Electron*., to be published. doi: 10.1109/TIE.2024.3352148.

[2] Y. Ma, D. Zhu, Z. Zhang, X. Zou, J. Hu and Y. Kang, "Modeling and transient stability analysis for Type-3 wind turbines using singular perturbation and lyapunov methods," *IEEE Trans. Ind. Electron*., vol. 70, no. 8, pp. 8075-8086, Aug. 2023.

[3] C. Wu, Y. Lyu, Y. Wang and F. Blaabjerg, "Transient synchronization stability analysis of grid-following converter considering the coupling effect of current loop and phase locked loop," *IEEE Trans. Energy Convers*., to be published. doi: 10.1109/TEC.2023.3314095.

[4] Y. Liu et al., "Transient stability enhancement control strategy based on improved PLL for grid connected VSC during severe grid fault," *IEEE Trans. Energy Convers.*, vol. 36, no. 1, pp. 218-229, Mar. 2021.

[5] B. Hu et al., "Synchronization stability enhancement of grid-following converter under inductive power grid," *IEEE Trans. Energy Convers*., vol. 38, no. 2, pp. 1485-1488, Jun. 2023.

[6] H. Wu and X. Wang, "Design-oriented transient stability analysis of PLL-synchronized voltage-source converters," *IEEE Trans. Power Electron*., vol. 35, no. 4, pp. 3573–3589, Apr. 2020.

[7] B. Hu, H. Nian, H. Li, L. Chen, S. Sahoo and F. Blaabjerg, "Impedance reshaping band coupling and broadband passivity enhancement for DFIG system," *IEEE Trans. Ind. Electron*., vol. 38, no. 8, pp. 9436-9447, Aug. 2023.

[8] X. Dong, Y. Zhao, W. Zhai, Z. Wang, K. Liu and G. Yan, "Group equivalent modeling and analysis of group subsynchronous oscillation of direct-drive wind turbine," in *5th International Electrical and Energy Conference (CIEEC)*, 2022, pp. 2661-2666.